Neoclassical tearing mode saturation in periodic current sheets

F. Militello,[1,2,a)] M. Ottaviani,[2] and F. Porcelli[1]
[1]*Burning Plasma Research Group and Politecnico di Torino, 10129 Torino, Italy*
[2]*Association Euratom CEA, CEA/DSM/IRFM, Cadarache, 13108 Saint-Paul-lez-Durance, France*

(Received 28 November 2007; accepted 3 March 2008; published online 14 April 2008)

The saturation of Neoclassical Tearing Mode islands in a periodic slab configuration is investigated. Several theoretical models, all based on a generalization of Rutherford's procedure, that aim at reducing the complete system to a single equation of the magnetic island width, are compared against numerical simulations. When the effects of the bootstrap current and of the second derivative of the equilibrium current profile are included, the numerical saturation levels are well matched with the predictions of this equation in a wide region of the stability diagram. However, the numerical results diverge from the standard theory when evaluating the threshold for nonlinear destabilization, since the theoretical value appears to be strongly conservative. In other words, the standard generalization of Rutherford's equation is not able to capture the minimum value of the linear stability parameter and of the island width such that below them the Neoclassical Tearing Mode is always suppressed. To correct this discrepancy, a new theoretical model in which the transverse propagation of the island affects the bootstrap current term is proposed. © *2008 American Institute of Physics*. [DOI: 10.1063/1.2901193]

I. INTRODUCTION

It is well known that magnetic reconnection processes, which allow changes in the topology of the magnetic field, can lead to enhanced transport and significant performance degradation of magnetic confinement devices. Of particular interest are the so-called Neoclassical Tearing Modes (NTMs). These occur because of a nonlinear mechanism that involves the modification of the bootstrap current in the region of magnetic islands of sufficiently large size. As a result, NTM islands can exist even for equilibria that are stable to ordinary tearing modes.

In recent years, several experiments have shown that advanced configurations for plasma confinement in tokamaks (Internal Transport Barrier, H-mode with Edge Localized Mode) may lead to the development of NTMs.[1,2] These magnetic perturbations may be harmful for the performance of the next generation tokamaks, which are envisaged to work in such regimes. In particular, when the island associated with the perturbation reaches a finite size, it can significantly reduce the radial confinement or even lead to plasma disruptions. Thus, the understanding of the evolution and the saturation of NTM islands has become a relevant issue for the magnetic fusion research community.

A distinctive characteristic of the Neoclassical Tearing instability is that nonlinear effects play an important role even in the early stage of its evolution. A simple model for the nonlinear evolution of the tearing mode, in the case of small Δ' equilibria, was first proposed by Rutherford.[3] The linear stability parameter, Δ' is defined in Ref. 4 as the jump of the logarithmic derivative of the fundamental eigenfunction of the perturbed magnetic flux around the reconnecting surface. In the standard linear theory it drives the instability growth when positive. The nonlinear solution obtained in Ref. 3 relies on a perturbative technique that is applicable when the island width, w, is small with respect to a macroscopic length, L. The smallness of the factor w/L allows a simplification of the problem by splitting the complete solution into two parts: a fully nonlinear inner solution, valid in a narrow layer around the reconnecting surface, and a linear outer solution, determined only by the equilibrium, the boundary conditions and the perturbation mode number, k. The matching of the two solutions in the region where they overlap yields the equation that governs the evolution of the island width.

From a technical point of view, the problem is therefore tackled by using an approach that aims at the reduction of the complex system of nonlinear partial differential equations to a single and simpler relation, where the only variable that characterizes the perturbation is the magnetic island width. Even if this procedure is fairly well suited to represent a basic model (e.g., the 2-equations model in Rutherford's paper), it may present shortcomings when trying to describe cases with pressure inhomogeneities, which add another important variable in the problem, the rotation frequency of the island, ω (see below).

In the original Rutherford's work, the island width equation has the simple form $dw/dt=\eta\Delta'$, the solution of which grows linearly in time. Therefore this equation does not deal with the tearing mode saturation. A satisfactory solution to the saturation problem was found only recently,[5,6] for the class of model equilibria, like the Harris pinch, that possess reflection symmetry around the reconnection surface. Following these results, the island width equation takes the form $dw/dt=\eta(\Delta'-\alpha w)$. Here η is the resistivity and α is a parameter that depends on the equilibrium current profile and which can be computed precisely from the theory. In the (Δ', w) plane, the stationary solution is represented by a

[a)]Present address: Institute for Fusion Studies, University of Texas, Austin, Texas 78712.

straight line going through the origin. In the rest of this paper, the plots showing the saturated island width as a function of the relevant physical parameter(s) are referred to as bifurcation diagrams.

The nonlinear theory of classic tearing modes was later extended to generic equilibria,[7–11] using various techniques. The outcome is a somewhat more complicated evolution equation for the island width. Note that in the literature, the evolution equation for the single degree of freedom given by the island width, is commonly refereed to as the generalized Rutherford's equation (GRE). As such, there are several versions of the GRE, depending on the included physical effects.

A fundamental result, described in Refs. 12–16, is that the GRE modified by the bootstrap current effect admits solutions with finite size saturated islands also for negative values of the linear stability parameter Δ'. Consequently, in a linearly stable regime, a so-called seed island, generated for instance by a sawtooth crash or the inhomogeneity of the coils, can grow and saturate if its width exceeds a threshold related to the plasma pressure gradient in the island region (which is proportional to the bootstrap current).

When more refined and complete models are concerned, the stability diagram shows a tangent bifurcation, so that for $\Delta' < \Delta'_{cr}$ (with $\Delta'_{cr} < 0$) a seed island is damped, whatever the value of its initial width. In the classical models, this stabilizing effect can be obtained by taking into account the parallel ion dynamics,[17–19] finite perpendicular transport,[15] or the polarization current.[20,21]

The introduction of the latter is particularly critical since it is associated with the poloidal rotation of the magnetic island. Indeed, the presence of pressure gradients implies that a minimal description of the island would require the knowledge of its rotation frequency, ω, besides its width, w. Therefore, even in the framework of the standard theories, a relation for the island width (GRE) is not sufficient to completely describe the physical problem and must be coupled to a relation that gives the rotation frequency. While the first can be computed following reduction procedures similar to the standard one, the latter represents an open theoretical issue. In this regard, it is useful to perform numerical calculations that can provide the dependence of the phase of the island with respect to time, and therefore ω.

In this work we numerically investigate the saturation of the Neoclassical Tearing Modes and we study the influence of the different physical effects by comparing our results with the theoretical models available in the literature. Furthermore, we propose a new mechanism for the stabilization of the NTMs associated with the effect of the island rotation on the bootstrap current contribution. The new theory is able to describe our numerical data better than the classic approach.

The paper is organized as follows: In Sec. II we describe the model equations we have used and the numerical code employed to solve them. Section III is dedicated to the discussion of the numerical results and their comparison with the standard analytical predictions of the GRE. In Sec. IV the mathematical procedure and the physical approximations that lead to the GRE are described. The bootstrap current contribution to the GRE is discussed in Sec. V, where also an alternative derivation is proposed. Finally, in Sec. VI, we draw our conclusion.

II. MODEL EQUATIONS AND NUMERICAL CODE

The physics of the NTMs can be described by a set of four equations that regulate the evolution of the magnetic flux, ψ, the electrostatic potential, φ, the perturbed electron density, n, and the ion velocity parallel to the magnetic field, v. These equations are reminiscent of those obtained by Hazeltine *et al.* in Ref. 22 and include a term that simulates the effect of the bootstrap current. Furthermore, the model takes into account electron diamagnetic effects that induce island rotation, the coupling with the ion sound waves, and allows for a finite Larmor radius. The electron temperature is assumed constant and the ions cold. The model is valid in 2D slab geometry and it is well suited to describe low-β, large aspect ratio magnetic fusion plasmas, where the confining magnetic field along the tokamak toroidal direction dominates over the other components,

$$\mathbf{B} = B_T \mathbf{e}_z + \nabla\psi \times \mathbf{e}_z, \tag{1}$$

with B_T, the guiding field along the ignorable direction, constant.

It is convenient to normalize all the variables in the model by using quantities that are relevant for the physical process we describe. In our convention, we assume that all the transverse length scales with L, a typical equilibrium length scale, and all the velocities with $v_A = (B_T \epsilon)/\sqrt{4\pi m_i n_c}$, the transverse Alfvén velocity. Here n_c is a typical density, m_i is the ion mass, and $\epsilon = L_x/L_y$ is the slab aspect ratio, evaluated with the numerical box sizes in the "radial" and "poloidal" directions, x, y. Consequently, the transverse Alfvén time is $\tau_A = L/v_A$. A natural normalization of the fields is as follows:

$$\hat{\varphi} = \frac{c}{L B_T v_A}\varphi, \tag{2}$$

$$\hat{\Psi} = \frac{1}{\epsilon L B_T}\Psi, \tag{3}$$

$$\hat{n} = \frac{d_i}{2L}\frac{\beta}{\epsilon}\frac{n}{n_c}, \tag{4}$$

$$\hat{v}_\parallel = \frac{d_i}{2L}\frac{v_\parallel}{v_A}, \tag{5}$$

where $d_i = c/\omega_{pi}$, $\omega_{pi} = e\sqrt{4\pi n_c/m_i}$ is the ion plasma frequency, and $\beta = 8\pi n_c T_e/B_T^2$ is the square of the ratio between the ion sound velocity and the Alfvén velocity. Therefore, the plasma vorticity and parallel current are (see Ref. 22)

$$\hat{U} = \tau_A U = \hat{\nabla}_\perp^2 \hat{\varphi}, \tag{6}$$

$$\hat{J}_z = \frac{4\pi L}{\epsilon c B_T} J_z = -\hat{\nabla}_\perp^2 \hat{\Psi}. \tag{7}$$

The model includes several dissipative effects such as the electrical resistivity, η, the particle diffusivity, D, the perpendicular ion viscosity, μ, and the parallel viscosity, χ. The normalized dissipative parameters are

$$\hat{\eta} = \frac{c^2 \tau_A}{4\pi L^2} \eta, \tag{8}$$

$$\hat{\mu} = \frac{\tau_A}{m_i n_c L^2} \mu, \tag{9}$$

$$\hat{\chi} = \frac{\tau_A}{m_i n_c L^2} \chi, \tag{10}$$

$$\hat{D} = \frac{\hat{\eta}\beta}{2}. \tag{11}$$

In the following, we decompose the density in a perturbed and equilibrium part, $\hat{n} = \hat{n}_{\mathrm{eq}}(x) + \tilde{\hat{n}}$, where the equilibrium is a function of x only. Note that, with this notation, $d\hat{n}_{\mathrm{eq}}/d\hat{r} = -v_*/v_A = -\hat{v}_*$, and $v_* = -(cT/eB_T n_c)(dn_{\mathrm{eq}}/dx)$ is the electron diamagnetic velocity.

Thus, the normalized equations are

$$dU/dt = [J, \psi] + \mu \nabla^2 U, \tag{12}$$

$$d\psi/dt = [n, \psi] - v_* \, \partial \psi/\partial y - \eta(J - J_{\mathrm{eq}} + J_b), \tag{13}$$

$$dn/dt + v_* \, \partial \phi/\partial y = \rho^2 [J, \psi] - \beta [v, \psi] + D\nabla^2 n, \tag{14}$$

$$dv/dt = -[n, \psi] + v_* \, \partial \psi/\partial y + \chi \nabla^2 v, \tag{15}$$

where n is the perturbed part of the density. Note that the hat notation as well as the subscript $\perp$, have been suppressed for simplicity and all quantities henceforth are to be considered as normalized. In Eq. (14) $\rho = \rho_s/L$, $\rho_s = c_s/\Omega$ with $c_s = \sqrt{T_e/m_i}$ the ion sound speed and $\Omega = eB_T/m_i c$ measures the ion gyrofrequency. The length reference scale is the radial dimension of the numerical box over 2π. The operator $[A, B] = \partial_x A \partial_y B - \partial_x B \partial_y A$ is the Poisson bracket, while $d\cdot/dt = \partial\cdot/\partial t + [\varphi, \cdot]$ contains the $\vec{E} \times \vec{B}$ drift.

The equilibrium magnetic flux function, generated by the equilibrium current density, is assumed to be $\psi_{\mathrm{eq}} = \cos(x)$. With this definition, J_{eq} includes the equilibrium part of the bootstrap current in addition to the equilibrium inductive current. On the other hand, the perturbed part of the bootstrap current is proportional to the radial derivative of the perturbed density, $J_b = c_b \partial_x n$, where c_b sets the strength of the bootstrap current. The equilibrium fields φ_{eq} and v_{eq} are assumed to be equal to zero.

The system of equations above has been solved numerically by employing a pseudospectral code which was already used in a similar analysis (see Ref. 17). The integration box has dimension $L_x \times L_y$ and is periodic in both directions. In the numerical integration we have used 256 harmonics to resolve the fields along the coordinate x and 8 in the y direction. The periodic boundary conditions impose that the wavevector is given by the expression,

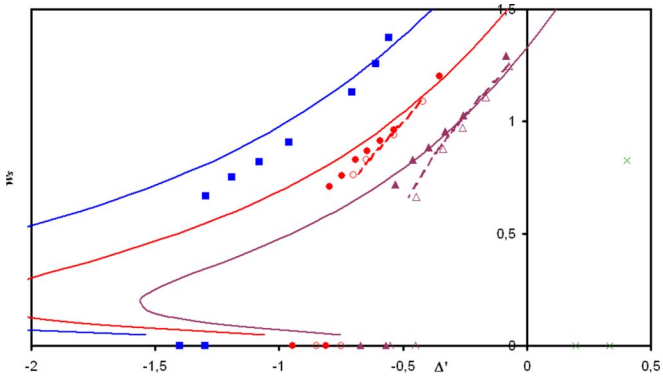

FIG. 1. (Color online) Bifurcation diagram. The solid lines represent the standard theoretical prediction of w_s, the saturated island width, for three different values of c_b [cf. Eq. (17)]. The numerical data with $c_b = 1$, $c_b = 1.4$, and $c_b = 2$ are represented with triangles, circles, and squares, respectively. Full symbols show cases with $\beta = 0.0025$ while for the empty symbols $\beta = 0$. A case with $c_b = 0$ is added for comparison (crosses). The dashed lines show the prediction of the new theory, where Δ_b is calculated using Eq. (26). The radial width of the numerical box is $L_x = 2\pi$.

$$k = m_0 \epsilon, \tag{16}$$

where m_0 is an integer number.

In order to understand the behavior of actual NTMs, the value of the parameters should be chosen to be as close as possible to that of a typical tokamak. The saturation time of the tearing mode is typically of the order of the resistive time. So, to keep the computation time reasonably short, we set $\eta = 10^{-3}$. As a consequence, also the other coefficients are rescaled so that their ratios are typical of a magnetically confined plasma. Thus, in all the simulations we have $\mu = \chi = 2 \times 10^{-4}$, $D = 5 \times 10^{-5}$, $\rho = 0.1$, $v_* = 0.1$, $\beta = 2.5 \times 10^{-3}$ or $\beta = 0$. Although the value of c_b is formally related to the values of β and ρ through the expression $c_b = 2.44(\beta/\epsilon)^{1/2}/\rho$, we consider it as a free parameter in order to study the bootstrap current effect on the saturation process. We varied it in the range $1 \le c_b \le 2$, which, however, are realistic values. Finally, by changing the aspect ratio, $\epsilon = L_x/L_y$, it is possible to modify the drive of the instability that acts on the magnetic islands. How to set Δ' in the code deserves a special discussion, that we give in Appendix A.

III. BEHAVIOR OF THE SYSTEM AND DISCUSSION OF THE STANDARD MODEL

In our analysis, we have investigated the stability diagram of the system for three different values of the bootstrap current parameter, $c_b = 1$, 1.4 and 2. The initial conditions of each field at the beginning of our numerical campaign were given by a stationary configuration including a finite size saturated island and characterized by $\Delta' = 0.405$ and no bootstrap current, $c_b = 0$ (cf. the cross in Fig. 1). Then, the system was taken to a new stability branch by increasing the value of the bootstrap current (by taking a finite value for c_b) and by decreasing the linear stability parameter (by increasing ϵ, as explained in Appendix A).

Without the effect of the bootstrap current and for the set of parameters used, a small reduction of Δ' from the starting point should lead to the loss of the magnetic island through

the β-stabilization described recently in Ref. 17. Therefore, our results show that, when c_b is large enough, it is possible to have a nonlinearly sustained island even where the parallel compressibility would lead to a stabilization (linear and nonlinear).

Once the new stable branch was reached, we gradually decreased the linear stability parameter until the system entered the linearly stable region, $\Delta' < 0$. Thus, in our simulations, the magnetic island is sustained by the bootstrap current even for negative values of Δ', in agreement with the theoretical predictions of the nonlinear behavior of the system.[12–16] However, the bootstrap current destabilization can maintain nonlinearly a finite size island only as long as the absolute value of the (negative) linear stability parameter does not exceed a threshold, Δ'_c, represented by a tangent bifurcation on the stability diagram. Despite the many works devoted to this issue, how to calculate the value of this threshold and the physical mechanisms involved in its determination, are still unclear from a theoretical point of view. Indeed, several models dealing with this problem have been investigated, most of them focusing on the effect of either cross-field transport or the polarization current.

The three values of c_b were scanned with the same *modus operandi*, in order to obtain a collection of information useful to scale the behavior of the system with the effect of the bootstrap current. In Fig. 1 we represent the numerical data for $c_b=1$ with triangles, $c_b=1.4$ with circles, and $c_b=2$ with squares. The shape of the stability diagram for the three cases treated is similar, while an increase of c_b, with all the other parameters fixed, corresponds to a more unstable configuration and, therefore, to a bigger magnetic island. In order to verify the analytic theory developed in Sec. V we have also performed simulations with $\beta=0$ (represented with empty triangles and circles for $c_b=1$ and $c_b=1.4$, respectively).

The most complete theoretical prediction of the system's behavior, relevant for the case treated here, can be obtained by including in the GRE the terms obtained in Refs. 5, 6, 12, 13, 15, and 21,

$$\Delta' = \Delta_{\mathrm{eq}} + \Delta_b + \Delta_p = -0.41bw - 6.34c_b v_* \frac{w}{w^2 + w_d^2} + \Delta_p(w, \omega, \ldots), \quad (17)$$

where b is the equilibrium current shape factor $[b = J_{\mathrm{eq}}(0)''/J_{\mathrm{eq}}(0)]$, $w_d = 1.8 w_c$ is defined in Ref. 15 and corresponds to the perpendicular transport effect, $\omega_* = k v_*$. The term called Δ_{eq} corresponds to the effect of the equilibrium current,[5,6] Δ_b is due to the bootstrap current,[12,13,15] while the last term, Δ_p, represents the contribution of the polarization current and depends on the structure of the plasma velocity field[20,21] through the island width, rotation frequency, and the plasma parameters.

We remark that the rotation frequency, ω, in the polarization term of Eq. (17) should be calculated self-consistently. However, a reliable theoretical expression for this quantity is not available in the literature, apart for cases in certain limits. In all our simulations, the rotation frequency of the island is slow, $O(0.1\omega_*)$, due to the almost complete flattening of the total density profile in the region inside the separatrix. This effect is also predicted in Refs. 21 and 23, where the ω relevant for our simulations should be exactly zero, since we have no electron viscosity. Therefore, in our comparison with the theory, we have neglected the polarization current effect.

The bootstrap current term in Eq. (17) requires particular attention since it applies only when the dominant mechanism for the evolution of the density is the diffusive transport and the inertial effects (such as the island rotation) can be neglected.[15] This is equivalent to assume a density conservation in the form,

$$D_{\parallel}[(n_{\mathrm{tot}}, \psi), \psi] + D\nabla_{\perp}^2 n_{\mathrm{tot}} \approx 0, \quad (18)$$

where $n_{\mathrm{tot}} = n - v_* x$ is the total density minus its value in $x=0$. The first term on the left-hand side of Eq. (18) gives the relevant parallel transport ($D_{\parallel}$ is a parallel diffusion coefficient), while the second gives the perpendicular transport. Note that $[(n_{\mathrm{tot}}, \psi), \psi] = \nabla_{\parallel}^2 n_{\mathrm{tot}}$ is the parallel Laplacian of the density. According to Ref. 15, the term w_d used in Eq. (17) is proportional to $(D/D_{\parallel})^{1/4}$.

We show now that our model contains transport physics such as that of Eq. (18) but it also includes other additional effects that modify the bootstrap current term, as discussed in the next section. While the perpendicular particle diffusion is transparent in our equations, the presence of parallel transport is much less obvious. The identification of the physics of the parallel diffusion is of great importance, since it induces the flattening of the density profile in the island region, thus fixing the poloidal rotation frequency of the island. The systems (12)–(15) contain two flattening mechanism, discussed below.

The first implicit parallel transport mechanism was discussed by Ottaviani *et al.* in Ref. 17. Note that, assuming negligible plasma flow, from the dominant balance in Eq. (13) the current density can be approximated by $J \approx \eta^{-1}[n_{\mathrm{tot}}, \psi]$. By substituting the thus-obtained expressions for J in Eq. (14) we find a term that is equivalent to the first term in Eq. (18), with $D_{\parallel} = \rho^2/\eta$. The second mechanism is related to the presence of ion sound waves in the system which lead to an enhanced parallel transport when $w > \rho^2 L_s / L_n = \rho v_* / \sqrt{\beta}$.[19,24] The analytic treatment of this effect is more delicate than that of the previous case and we will address it here only qualitatively. Assuming again small inertial effects, from Eq. (15) we have that $v \approx (\chi k_{\perp}^2)^{-1}[n_{\mathrm{tot}}, \psi]$. Substituting the previous expression in Eq. (14) we can estimate that $D_{\parallel} \approx \beta w^2/\chi$, where the island width was taken as the characteristic transverse length of the perturbations. The total parallel diffusion coefficient is produced by the simultaneous occurrence of the two mechanisms described above, so that $D_{\parallel} = D_{\parallel 1} + D_{\parallel 2}$. As a consequence, in our simulations $w_d \cong 0.19$ when $\beta = 0.0025$ and $w_d \cong 0.23$ when $\beta = 0$. Note that this corresponds to a ratio of parallel to cross-field particle transport of the order of 10^5.

As shown in Fig. 1, the analytic predictions given by the GRE reduced in this way, are in good agreement with our numerical results for a wide range of Δ'. On the other hand, the theoretical model shows several points of weakness. In

particular, it is not very accurate for large values of w and c_b and, most importantly, it fails to predict the correct position of the tangent bifurcation (see Fig. 1).

The lack of precision for large w is easily justified by the observation that the GRE is obtained by employing a perturbative expansion in the island width. Thus, if the island becomes too big, $w/L \simeq 1$, the nonlinear solution is no longer valid. Finite island size effects should be taken into account and an extra term, proportional to w^3, should be added in Eq. (17). Also, the discrepancy between theory and numerical results when c_b is large can be explained by a limit of the model. Indeed, a key assumption in the treatment of the nonlinear systems (12)–(15) is that the constant-ψ approximation remains valid in the nonlinear regime as well (see Ref. 3). This implies that the GRE is valid as long as $|\Delta' w| \ll 1$. When the bootstrap current parameter is too large, the saturated island width becomes of the order of Δ'^{-1} and the constant-ψ approximation is no longer correct.

The problem of the accuracy of the prediction of the tangent bifurcation is more complicated. Within the theoretical model used, Eq. (17), the tangent bifurcation is generated by the effect of the cross-field transport in the bootstrap current term and by the polarization current term. However, the former effect becomes relevant for only very small islands, $w \sim w_d$, while the latter should go exactly to zero, following the present day theories. This disagreement between numerical data and standard predictions requires a more detailed investigation of the validity of the assumptions employed in the derivation of Eq. (17). Our results also show that small islands present a rotation frequency which can become as large as 30% of the electron diamagnetic frequency before the island collapses at the tangent bifurcation. This suggests that new inertial effects could be responsible for the lack of precision of the standard model close to the critical point. In the next sections we will describe the analytical technique used to obtain the GRE and we will propose an alternative theoretical explanation to cure the observed discrepancy based on the effect of the island rotation on Δ_b.

IV. THEORETICAL ANALYSIS

In the following we shortly describe the method to obtain the GRE. The standard procedure requires the calculation of the total nonlinear current, which can be related to the linear stability parameter through the expression[3]

$$\Delta' = (\tilde{\psi}\pi)^{-1} \int_{-\infty}^{\infty} dx \oint d(\epsilon y) J \cos(\epsilon y), \tag{19}$$

where $\tilde{\psi}$ is the value of the fundamental ($n_0=1$) eigenfunction of ψ calculated in $x=0$. In order to obtain the nonlinear current, J, we need to reduce the equations of our system.

The saturated configurations are in steady state, which implies that all the time derivatives can be set to zero in the island frame of reference. Then, the magnetic flux surfaces average of Eq. (13) gives

$$\langle J \rangle_\psi = \langle J_{\rm eq} \rangle_\psi - \langle J_b \rangle_\psi, \tag{20}$$

which is the part of the current that depends only on

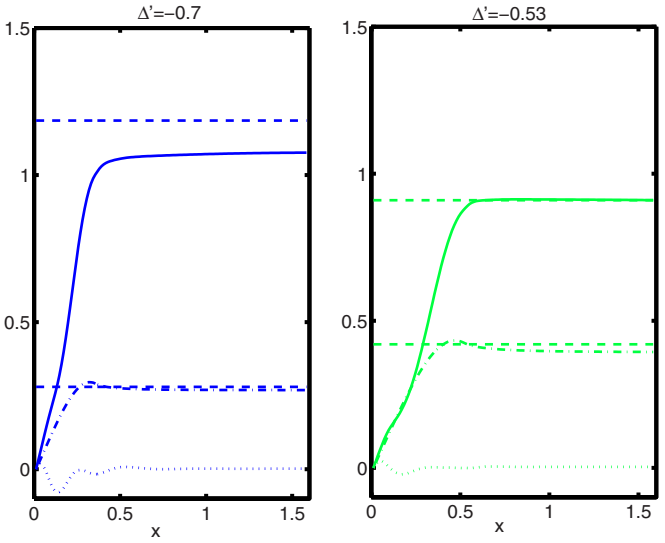

FIG. 2. (Color online) Numerical asymptotic matching of Δ_b (solid curve), $\Delta_{\rm eq}$ (dashed-dotted curve), and Δ_p (dotted curve) for $c_b=1.4$, $\beta=0$. Δ' is -0.7 for the left plot and -0.53 for the right plot. The dashed curves indicate the theoretical values of Δ_b and $\Delta_{\rm eq}$ calculated using Eq. (17).

ψ [$\langle \cdots \rangle_\psi = (2\pi)^{-1} \oint d(\epsilon y) \cdots |_{\psi=\text{const}}$]. We proceed by observing that from Eq. (13) we have for small resistivity,

$$n_{\rm tot} \cong \varphi + H(\psi), \tag{21}$$

where $H(\psi)$ is an unknown function that can be obtained by solving the higher order transport equations (for all the details, see Ref. 21). Here φ represents the ion stream function (or equivalently the electrostatic potential) in the island frame of reference. Substituting Eq. (21) in Eq. (14) and integrating over ψ, we find

$$J = I(\psi) + \frac{H'(\psi)}{\rho^2}\varphi - \frac{\beta}{\rho^2} v, \tag{22}$$

where the prime indicates derivation with respect to ψ. For small χ, Eq. (15) gives $v = \psi + G(\varphi)$, where $G(\varphi)$ is due to the integration and can be found by solving the transport equations. From Eqs. (20) and (22) we find that

$$J\langle 1 \rangle_\psi = \langle J_{\rm eq} \rangle_\psi - \langle J_b \rangle_\psi + \frac{H'(\psi)}{\rho^2}(\varphi\langle 1 \rangle_\psi - \langle \varphi \rangle_\psi)$$

$$- \frac{\beta}{\rho^2}[G(\varphi)\langle 1 \rangle_\psi - \langle G(\varphi) \rangle_\psi]. \tag{23}$$

We call polarization current the total current minus its flux surface average, i.e., $J_{\rm pol} = J - \langle J \rangle_\psi / \langle 1 \rangle_\psi$, and it is given by the last four terms on the right-hand side of Eq. (23). Replacing the previous equation into Eq. (19), we obtain the GRE.

V. DISCUSSION OF THE BOOTSTRAP AND POLARIZATION CURRENT EFFECTS

In this section we discuss the last two terms in Eq. (17) and propose a new expression for Δ_b. In order to identify the origin of the observed discrepancy between our numerical results and the standard predictions, it is useful to isolate and analyze the single contributions to the GRE. This can be done by numerically evaluating the different currents in Eq.

(23), substituting the outcome in Eq. (19), and therefore performing a "numerical asymptotic matching," the results of which are Δ_{eq}, Δ_b, and Δ_p. These quantities and their theoretical counterparts, predicted with Eq. (17) for $c_b=1.4$, $\beta=0$, are plotted in Fig. 2 for two different values of Δ' (−0.7 and −0.53). Our analysis confirms that, for large islands, the standard models accurately describe the equilibrium and bootstrap effect, while the polarization current term is small and therefore negligible compared to the others. At the same time, for smaller and faster islands, we find that while the theoretical Δ_{eq} agrees with the numerical data and Δ_p can still be neglected, the predicted Δ_b is larger then the actual numerical value. This is a clear indication that the bootstrap term calculated in Refs. 12, 13, 15, and 16 is not adequate to describe the complex behavior of small rotating islands. Furthermore, this comparison rules out the possibility that the polarization term can significantly modify the position of the tangent bifurcation and confirms that, in first approximation, it is correct to neglect it.

These observations justify a more detailed investigation of the bootstrap term and the inclusion of inertial effects in the calculation. We remark that $J_b=c_b\partial_x n=c_b\left[v_*+\partial_x\varphi+\partial_x\psi\left(dH/d\psi\right)\right]$, where the density perturbation has been expressed using Eq. (21). As a first step, we calculate the profile function H, following the procedure described in Ref. 21. This can be done by averaging Eq. (14) over the magnetic flux surfaces, observing that $[\varphi,n_{tot}]=\nabla\cdot(n_{tot}\mathbf{v})$ and using the property $\langle\nabla\cdot\mathbf{\Gamma}\rangle_\psi=d/d\psi\langle\Gamma\cdot\nabla\psi\rangle_\psi$. We obtain

$$\langle\varphi[n_{tot},\psi]\rangle_\psi+D\langle\nabla n_{tot}\cdot\nabla\psi\rangle_\psi=C_1, \tag{24}$$

where the constant C_1 can be determined by applying the correct boundary conditions as shown in Appendix B. Equation (24) describes the same density transport physics as Eq. (18) and, in addition, includes convection. The first term on the left-hand side of the previous equation can be evaluated by taking the flux surface average of Ohm's law multiplied by φ, $\langle\varphi[n_{tot},\psi]\rangle_\psi=\eta\langle\varphi(J-J_{eq}+J_b)\rangle_\psi$ and using Eq. (23) to evaluate the current. Thus, we find

$$\frac{dH}{d\psi}=\frac{C_2-\langle\nabla\varphi\cdot\nabla\psi\rangle_\psi+\frac{\eta}{D}\{J_{eq}\}-\frac{\eta c_b}{D}\left\{\frac{\partial\varphi}{\partial x}\right\}-\frac{\eta\beta}{\rho^2 D}\{G(\varphi)\}}{\langle|\nabla\psi|^2\rangle_\psi+\frac{\eta}{\rho^2 D}\{\varphi\}+\frac{c_b\eta}{D}\left\{\frac{\partial\psi}{\partial x}\right\}}\Theta, \tag{25}$$

where $C_2=C_1/D$,

$$\{\cdots\}=\langle\varphi\cdots\rangle_\psi-\frac{\langle\varphi\rangle_\psi\langle\cdots\rangle_\psi}{\langle 1\rangle_\psi},$$

and Θ is a step function that takes the value 0 inside the separatrix and 1 outside. As a standard approximation, when the island is small with respect to a macroscopic scale, we will take $|\nabla\psi|^2\cong x^2$.

For sake of simplicity, we assume that $\varphi=-vx$ in the island frame of reference, with $v=\omega/k$. This is equivalent to neglecting the plasma response to the presence of the island in favor of the flow generated by the mode rotation. With this *ansatz* the magnetic flux averages can be calculated in terms of elliptic integrals. Furthermore, in the analytic treatment we take $\beta=0$, thus simplifying the solution. An extension to finite β will be the subject of future work. After some algebra (detailed in Appendix C) we find that

$$\Delta_b=\frac{v_* c_b}{w}4\pi\int_1^\infty d\Omega\left\{\sqrt{\frac{2}{\Omega+1}}\left[\frac{(1+\Omega)E-\Omega K}{K}\right]\frac{\frac{C_2}{v_*}-\frac{v}{v_*}+\frac{v}{v_*}\frac{\eta}{D}\frac{w^2}{16}\left[\Omega-\frac{(\Omega+1)E}{K}\right]}{E-\frac{v}{v_*}\frac{\eta}{D}\left(c_b v_*+\frac{v_*^2}{\rho^2}\frac{v}{v_*}\right)\left(E-\frac{\pi^2}{4}\frac{1}{K}\right)}\right\}, \tag{26}$$

where $\Omega=(1-\psi)/\tilde{\psi}$, $K=K\left[2/(\Omega+1)\right]$, and $E=E\left[2/(\Omega+1)\right]$ are elliptic integrals of the first and second kind.

To discuss the previous expression, without loss of generality, we use the standard boundary condition applied in Refs. 12–16, where the particle flux matches the equilibrium value for large x, which implies $C_2=v_*$. The extension to the periodic boundary domain associated with our numerical box, where this approximation is no longer valid, and the calculation of the relevant form of C_2 are discussed in details in Appendix B. First of all, note that once the physical pa-

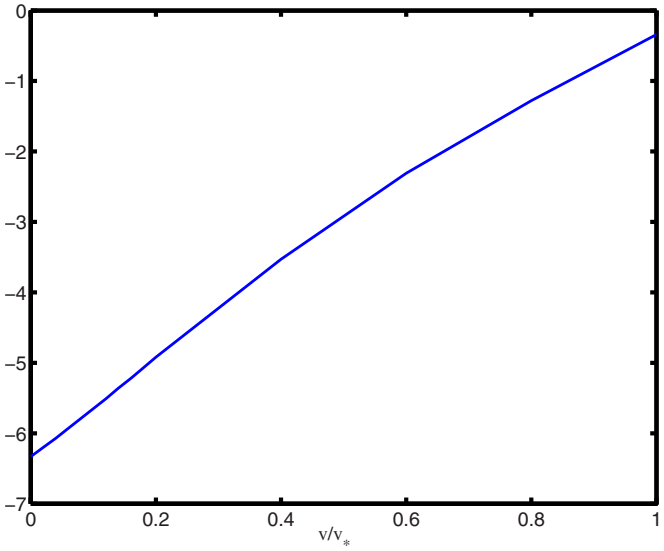

FIG. 3. (Color online) The curve represents the coefficient that multiplies $v_* c_b / w$ in Eq. (26) as a function of v/v_*. For the case shown $c_b=1$, $w=1$ and $C_2=v_*$.

rameters are fixed, the right-hand side of Eq. (26) is a complicated function of w and of v/v_*. In Fig. 3 we show the behavior of the numerical value multiplying $c_b v_*/w$ in Eq. (26) as a function of the rotation frequency for $c_b=1.4$ and $w=1$ (the dependency on w and c_b is very weak). We emphasize that, even for islands with a relatively slow rotation, the bootstrap term can be reduced by a significant fraction. For example, when v is 20% of the diamagnetic velocity, Δ_b decreases by 25%.

Finally, we show that our solution contains the standard non inertial limit. When φ is negligible (i.e., v/v_* small), the expressions (21) and (25) reduce to

$$\frac{dH}{d\psi} = \left(\frac{\partial n_{\mathrm{tot}}}{\partial \psi}\right)_{\mathrm{standard}} = \frac{1}{w}\sqrt{\frac{2}{\Omega+1}}\frac{\pi C_2}{E}, \tag{27}$$

which is equivalent to Eq. (41) in Ref. 15 for the standard boundary conditions $C_2=v_*$. Similarly, Eq. (26) becomes

$$\Delta_b = -6.34\alpha(w)\frac{v_* c_b}{w}. \tag{28}$$

Here $\alpha(w)=C_2/v_*$ is a correction factor expressing the fact that for the periodic domain associated with our numerical box, the boundary conditions for Eq. (24) must be different from those in Refs. 12–16. The mathematical details of the derivation of α, which can be obtained through a fully analytical procedure, are given in Appendix B. For $w \ll 1$ we have that $\alpha \to 1$ and we retrieve the standard limit of Refs. 12–16, that does not include neither inertial nor perpendicular diffusivity effects (introduced by Fitzpatrick by means of a Padé approximation).

VI. CONCLUSIONS

In the last 15 years a strong theoretical effort has been spent to tackle the problem of the NTM evolution and saturation. To achieve an analytical solution, all the models developed rely on simplified physics and on strong assumptions. On the other hand, by approaching the question with numerical tools it is possible to solve the complete set of equations. Then, a systematic numerical investigation can shed some light on the validity of each theory and give a more global view of the behavior of the system.

Our results show a good agreement with the classical analytical curves obtained by solving the standard GRE only for slowly rotating large islands. In particular, it is found that to obtain reliable predictions for the saturated island size it is sufficient to take into account the effects of the shape of the equilibrium current density and of the bootstrap current. The effect of the polarization current can be neglected according both to the theory, which gives a vanishing ω, and to the simulations. However, the standard GRE, Eq. (17), is a good approximation only far from the tangent bifurcation, since in the neighborhood of the critical point the bootstrap term takes a different form with respect to those given in Refs. 12–16.

Indeed, our simulations yield that a prediction based on the standard generalized Rutherford equation is not able to capture the position of the tangent bifurcation in the stability diagram, which defines the threshold for the nonlinear destabilization of the mode. We propose that, in the model under study, and for the parameter range under consideration, the cause of this departure from the standard analytic theory is due to the effect of the island rotation that reduces the destabilizing effect of the bootstrap current term.

Since our study has been carried out in a simplified slab geometry and with certain physical parameters constrained by numerics, it is useful to discuss to what extent our results may be extrapolated to a more realistic situation. As already noted, in our study, the ratio of parallel to cross-field particle transport is of the order of 10^5. In an actual machine, this ratio would be substantially higher, when evaluated within collisional theory; this would implies a reduction of the seed island w_d of a couple of orders of magnitude. As a consequence, the effect of the polarization current, which in slab geometry grows rapidly when the island width is comparable to the ion sound Larmor radius, could become comparable to the effect of the island rotation frequency on the bootstrap term. We also remark that in toroidal geometry, the polarization current effect could be further enhanced by the fact that it scales like the square of the banana orbit width, w_b, rather then the square of the ion sound Larmor radius. Since $w_b/\rho_s \approx q(T_i/T_e)^{1/2}/\epsilon^{1/2}$,[25] where q is the safety factor, T_i and T_e the ion and electron temperatures and ϵ is the local inverse aspect ratio, we expect this enhancement to be of one–two orders of magnitude. However, this modification may not significantly affect our results since, on the basis of the simulations presented in this paper, the polarization current effect is typically three–four orders of magnitude smaller than the bootstrap current effect (see Fig. 2). A further uncertainty is due to the fact that perpendicular transport in a realistic plasma is likely due to turbulence. This may justify the use of enhanced perpendicular transport coefficients, as long as the width of the island is larger than the characteristic scale length of the turbulent eddies (see Ref. 26, and references therein). This scale length would be typically of the

order of a few Larmor radii. On the other hand, the very existence of a sufficiently large island, with nearly flat gradients, would alter the nature of the turbulence, which relies on those gradients as a driving agent. Little information is known in this respect, and this makes it difficult to evaluate how much the perpendicular transport coefficients should be increased to emulate a more realistic situation. In order to satisfactorily answer this question it is probably necessary to carry out multiscale simulations in 3D geometry with very long integration times that would cover all the necessary spatial and time scales, a daunting task. In the end, how much the rotation of the island can affect the bootstrap current drive of neoclassical tearing modes may depend on the nature of the perpendicular transport mechanism.

ACKNOWLEDGMENTS

The authors are happy to acknowledge fruitful discussions with Dr. R. J. Hastie and Dr. F. L. Waelbroeck. F.M. is grateful to Dr. E. Asp for a careful reading of the manuscript.

APPENDIX A: BREAKING OF THE SYMMETRY BY THE BOOTSTRAP CURRENT AND CALCULATION OF Δ'

We first emphasize that the equilibrium used in our simulations generates three reconnecting surfaces, at $x=0, \pm\pi$, where the tearing mode develops and the associated magnetic islands can grow. If the islands have a small width with respect to L_x it is reasonable to assume that they do not directly interfere with each other's evolution. That means that each island can be considered as a single isolated entity, and its growth and saturation are determined only by the parameters and by the local value of Δ'. However, this assumption does not imply that the perturbations are completely magnetically decoupled. Indeed, while the physics of the nonlinear layers around the reconnecting surfaces is unaltered, the linear outer solution between the islands, $\tilde{\psi}_{\mathrm{out}}$, must be calculated by using self-consistent boundary conditions, and is thus dependent on the island widths. We remark that $\tilde{\psi}_{\mathrm{out}}$ is the fundamental component of the Fourier decomposition of the perturbed magnetic flux. It follows that the central island (at $x=0$) is affected by the edge islands (at $x=\pm\pi$) because the presence of the latter contributes to the definition of the boundary conditions at $x=\pm\pi$ of the equation for $\tilde{\psi}_{\mathrm{out}}$,

$$\frac{d^2\tilde{\psi}_{\mathrm{out}}}{dx^2} - (k^2-1)\tilde{\psi}_{\mathrm{out}} = 0, \tag{A1}$$

which is the linearized version of Eq. (12). Due to the particular choice of the equilibrium, it is possible to analytically solve the previous equation, that, for $0 \le x \le \pi$, gives

$$\tilde{\psi}_{\mathrm{out}} = A\cos[\tilde{k}(x-\pi/2)] + B\sin[\tilde{k}(x-\pi/2)],$$
$$\tilde{k} = \sqrt{k^2-1} < 0, \tag{A2}$$

$$\tilde{\psi}_{\mathrm{out}} = A'\cosh[\tilde{k}(x-\pi/2)] + B'\sinh[\tilde{k}(x-\pi/2)],$$
$$\tilde{k} = \sqrt{k^2-1} > 0, \tag{A3}$$

where A, B, A', and B' are constants of integration.

The complete solution, with the constant of integration determined, can be obtained by solving a four-equation system. In particular, if we take the case $\tilde{k}<0$, we have (for $\tilde{k}>0$ the calculation follows similar lines)

$$\tilde{\psi}_c = A\cos[\tilde{k}(\pi/2)] - B\sin[\tilde{k}(\pi/2)], \tag{A4}$$

$$\tilde{\psi}_e = A\cos[\tilde{k}(\pi/2)] + B\sin[\tilde{k}(\pi/2)], \tag{A5}$$

$$\tilde{\psi}'_c = A\tilde{k}\sin[\tilde{k}(\pi/2)] + B\tilde{k}\cos[\tilde{k}(\pi/2)], \tag{A6}$$

$$\tilde{\psi}'_e = -A\tilde{k}\sin[\tilde{k}(\pi/2)] + B\tilde{k}\cos[\tilde{k}(\pi/2)], \tag{A7}$$

where a prime represents a derivative with respect to x, $\tilde{\psi}_c$, and $\tilde{\psi}_e$ are the values of the fundamental eigenfunction of the perturbed magnetic flux for $x=0$ (the central island), and for $x=\pi$ (the edge island), respectively. We emphasize that, in order to obtain A and B, two equations are not sufficient. Indeed, the values of $\tilde{\psi}_{c,e}=w^2_{c,e}/16$ (valid for this equilibrium) are related to the magnetic island widths, which are not known *a priori*. They can be calculated by employing a GRE-like approach, i.e., by using the expression of the nonlinear current density in the edge and central boundary layer to evaluate $\tilde{\psi}'_{c,e}$.

The nonlinear current is easily obtained by averaging Eq. (13) over the magnetic flux surfaces,

$$J = \langle J_{\mathrm{eq}}(x)\rangle + c_b\left\langle\frac{\partial n}{\partial x}\right\rangle - \eta^{-1}\left\langle\frac{\partial\psi}{\partial t}\right\rangle + J_p, \tag{A8}$$

where J_p is due to the fact that the inertia is taken into account in Eq. (12), $[J,\psi]\neq 0$, and is related to the polarization current effect. We are reminded that the averaging operator can annihilate the Poisson bracket that contains the magnetic flux, $\langle[f,\psi]\rangle=0$, where f is a periodic function of ξ. The definition of this average is given, for example, in Ref. 5. Finally, from Ampere's law we have that $\tilde{\psi}'_{c,e}=0.5\pi^{-1}[\int_{-\infty}^{\infty}dx'\oint d\xi\cos\xi J(x',\xi)]_{c,e}$, where the subscripts c and e indicate that the integral is computed around the central or edge nonlinear boundary layers, respectively. The infinity symbol means that the limit of integration is far from the reconnecting surface (the integrand goes to zero quickly outside the boundary layers).

As a first approximation, we assume that the polarization current effect is negligible and we use a stationary magnetic flux, since we are interested in the saturation. Consequently, we have that

$$\tilde{\psi}'_{c,e} \cong \frac{1}{2\pi}\left[\int_{-\infty}^{\infty} dx' \oint d\xi \cos\xi \langle \cos x\rangle\right]_{c,e} + \frac{c_b}{2\pi}\left[\int_{-\infty}^{\infty} dx' \oint d\xi \cos\xi \left\langle \frac{\partial n}{\partial x}\right\rangle\right]_{c,e}. \tag{A9}$$

The integrals in the above equation can be computed numerically. Note that the second integral function in Eq. (A9) takes the same value either in $x=\pm\pi$ and in $x=0$. Conversely, the first integral evaluated on the central and edge reconnecting surfaces, changes sign, as can be understood by analyzing the integrand. Therefore, we have

$$\tilde{\psi}'_c = \mathcal{C}_{\rm eq}\tilde{\psi}_c^{3/2} + c_b\mathcal{C}_b\tilde{\psi}_c^{1/2}, \tag{A10}$$

$$\tilde{\psi}'_e = -\mathcal{C}_{\rm eq}\tilde{\psi}_c^{3/2} + c_b\mathcal{C}_b\tilde{\psi}_c^{1/2}, \tag{A11}$$

where $\mathcal{C}_{\rm eq}=0.82$ and $\mathcal{C}_b=-0.79v_*$ are the result of the numerical integration. To calculate $\mathcal{C}_b$ we made use of the theoretical perturbed density profile given in Ref. 15, with $w_c=0$.

It is useful to introduce two alternative variables for the perturbed magnetic flux, $\delta_+=\sqrt{\tilde{\psi}_e}+\sqrt{\tilde{\psi}_c}$ and $\delta_-=\sqrt{\tilde{\psi}_e}-\sqrt{\tilde{\psi}_c}$. With this notation, substituting Eqs. (A10) and (A11) in the systems (A4)–(A7), we have

$$(\delta_+^2+\delta_-^2)\tilde{k}\tan[\tilde{k}(\pi/2)] = \mathcal{C}_{\rm eq}\frac{\delta_+^3+3\delta_-^2\delta_+}{2} - 2c_b\mathcal{C}_b\delta_-, \tag{A12}$$

$$\delta_+\delta_-\tilde{k}\cot[\tilde{k}(\pi/2)] = -\mathcal{C}_{\rm eq}\frac{\delta_-^3+3\delta_+^2\delta_-}{4} + c_b\mathcal{C}_b\delta_+. \tag{A13}$$

Finally, if we multiply Eqs. (A12) and (A13), we obtain

$$-8\delta_+\delta_-(\delta_+^2+\delta_-^2)\tilde{k}^2 = \mathcal{C}_{\rm eq}^2\delta_+\delta_-(\delta_+^2+3\delta_-^2)(\delta_-^2+3\delta_+^2) + 16c_b^2\mathcal{C}_b^2\delta_+\delta_- - 4c_b\mathcal{C}_b\mathcal{C}_{\rm eq}(\delta_+^4 + 6\delta_+^2\delta_-^2+\delta_-^4). \tag{A14}$$

Solving Eqs. (A12) and (A13) allows us to obtain the values of the magnetic island widths on the two reconnecting surfaces, while Eq. (A14) provides useful information on the final state of the two islands. For example, in the limit $c_b=0$, we find that $\delta_-=0$ is the only physical solution of the system. Indeed, if $\delta_-\neq 0$ the values of the magnetic island widths would be imaginary. As a consequence, when the bootstrap current is not present, the island on the central reconnecting surface has the same width as the one on the edge resonant surface ($\delta_-=0$), $B=0$ and the island width is given by the usual analytic expression,

$$2\tilde{k}\tan[\tilde{k}(\pi/2)] = \mathcal{C}_{\rm eq}\delta_+, \tag{A15}$$

which is equivalent to $\Delta'=0.41w$ (see Refs. 5 and 6).

Thus, by changing the aspect ratio, $\epsilon=L_x/L_y$, it is possible to modify the drive of the instability that acts on the magnetic islands [cf. Eq. (16)]. The situation becomes more complex in the presence of the bootstrap current effect. When $c_b\neq 0$ a symmetry breaking term is introduced in Eq. (A14). Consequently, the $\delta_-=0$ is no longer a solution of the system and the island on the edge is typically smaller than the island in the central resonance. Therefore, to determine the outer magnetic flux and the island widths the solution of the systems (A12) and (A13) is required. Thus, we have proved that there is a magnetic connection between the central and edge resonances, although the width of each island is fixed only by the local value of Δ'.

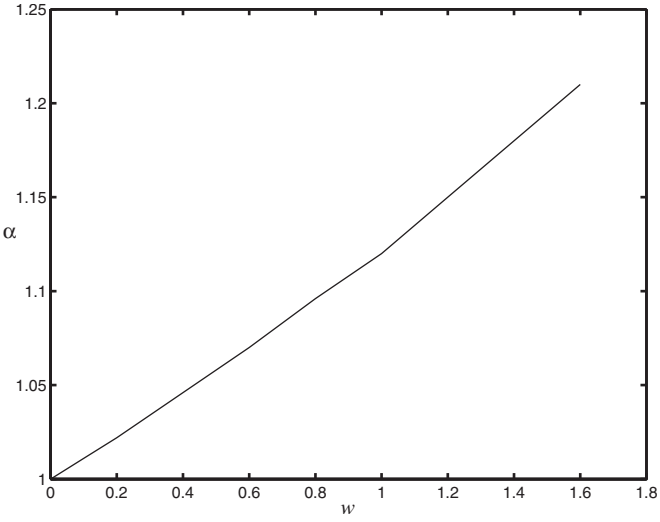

FIG. 4. Plot of the dependence of α with respect to the island width,w, Eq. (B4).

In our simulations, we have changed the aspect ratio, ϵ, and evaluated *a posteriori* the linear stability parameter through a best fit analysis of the numerical results.

Finally, we remark that the polarization current term, the time dependent term, or any other term with an integrand that changes its sign on the two resonances, would behave like the first term on the right-hand side of Eq. (A9). As a consequence, they would not break the symmetry and $\delta_-=0$ would remain a solution of the system.

APPENDIX B: DENSITY PROFILE WITH PERIODIC BOUNDARY CONDITIONS

In this Appendix we evaluate the effect of periodic boundary conditions on the calculation of the bootstrap current term in the Generalized Rutherford equation.

In the standard theory,[12,13,15,16] the integration constant in Eq. (25) is obtained by imposing that the particle flux far from the resonant surface matches the equilibrium one, $\partial_x n_{\rm tot}=\partial_x n_{\rm eq}=-v_*$ at $x\to\infty$. Similarly, we have that $\partial_x\varphi=-v$ at $x\to\infty$. As $d_\psi H=\partial_x(n-\varphi)/\partial_x\psi$, the right-hand side of Eq. (25) has to go like $(v_*-v)/x$ asymptotically. Following the approximations of the text, $\varphi\approx -vx$ and $\beta=0$, we can express Eq. (25) in terms of elliptic functions, as described in Appendix C. The asymptotic behavior of the right-hand side of Eq. (25) is therefore given by the following expression:

$$\lim_{x\to\infty}\frac{dH}{d\psi} = \frac{C_2-v}{x}, \tag{B1}$$

from which we deduce that $C_2=v_*$.

The standard boundary conditions do not accurately describe the problem when dealing with a periodic domain. Indeed, in this case magnetic islands grow around the edge resonances at $x=\pm\pi$ and inside their separatrices, where $\Omega=\Omega_e\approx 8\pi^2/w_c^2$, the density is equal to the equilibrium value, $n_{\mathrm{tot}}(\Omega_e)=\pm n'_{\mathrm{eq}}(x=0)\pi$. The density in the central island is approximately constant and hence on the separatrix, where $\Omega=1$, we have that $n_{\mathrm{tot}}(\Omega=1)=0$ [remember that we assume, without loss of generality, that $n_{\mathrm{eq}}(x=0)=0$]. Therefore, in order to find the integration constant C_2 we must satisfy the relation,

$$n(x=\pi)-\varphi(x=\pi)=-\pi(v_*-v)=-\frac{w^2}{16}\int_1^{\Omega_e}d\Omega\frac{dH(\Omega)}{d\psi}, \tag{B2}$$

where $dH/d\psi$ is given again in Appendix C. As a result, we have

$$\frac{C_2}{v_*}=\frac{v}{v_*}+\frac{B_2}{\displaystyle\int_1^{\Omega_e}d\Omega\left[\sqrt{\frac{2}{\Omega+1}}\frac{1}{E-B_1\left(E-\frac{\pi^2}{4}\frac{1}{K}\right)}\right]}-B_3\frac{\displaystyle\int_1^{\Omega_e}d\Omega\left[\sqrt{\frac{2}{\Omega+1}}\frac{\Omega-\frac{(\Omega+1)E}{K}}{E-B_1\left(E-\frac{\pi^2}{4}\frac{1}{K}\right)}\right]}{\displaystyle\int_1^{\Omega_e}d\Omega\left[\sqrt{\frac{2}{\Omega+1}}\frac{1}{E-B_1\left(E-\frac{\pi^2}{4}\frac{1}{K}\right)}\right]}, \tag{B3}$$

where

$$B_1=\left(\frac{v_*^2}{\rho^2}\frac{v}{v_*}+c_b v_*\right)\frac{\eta}{D}\frac{v}{v_*},$$

$$B_2=\left(1-\frac{v}{v_*}\right)\frac{16}{w},$$

and

$$B_3=\frac{\eta}{D}\frac{v}{v_*}\frac{w^2}{16}.$$

It is interesting to evaluate the limit of Eq. (B3) for negligible rotation velocity,

$$\lim_{v\to 0}\frac{C_2}{v_*}=\alpha(w)=\frac{8\sqrt{2}}{w\displaystyle\int_1^{8\pi^2/w^2}d\Omega(\Omega+1)^{-1/2}E^{-1}}, \tag{B4}$$

which is a growing function of w and goes to 1 when $w\to 0$, as can be seen in Fig. 4.

APPENDIX C: CALCULATION OF Δ'

In this Appendix we give the mathematical details of the calculation of the expression for Δ_b given in Eq. (26). Following the text, we assume that $\beta=0$ and $\varphi=-vx$. The former approximation implies $\{\cdots\}=-v\left(\langle x\cdots\rangle_\psi-\frac{\langle x\rangle_\psi\langle\cdots\rangle_\psi}{\langle 1\rangle_\psi}\right)$. As a consequence, we can write the terms within curly brackets in Eq. (25) as

$$\{J_{\mathrm{eq}}\}=\{1\}-\left\{\frac{x^2}{2}\right\}=v\left(\left\langle\frac{x^3}{2}\right\rangle_\psi-\frac{\langle x\rangle_\psi\left\langle\frac{x^2}{2}\right\rangle_\psi}{\langle 1\rangle_\psi}\right), \tag{C1}$$

$$\left\{\frac{\partial\varphi}{\partial x}\right\}=-v\{1\}=0, \tag{C2}$$

$$\{\varphi\}=-v\{x\}=v^2\left(\langle x^2\rangle_\psi-\frac{\langle x\rangle_\psi^2}{\langle 1\rangle_\psi}\right), \tag{C3}$$

$$\left\{\frac{\partial\psi}{\partial x}\right\}=-\{x\}=v\left(\langle x^2\rangle_\psi-\frac{\langle x\rangle_\psi^2}{\langle 1\rangle_\psi}\right), \tag{C4}$$

where the first two terms of the local Taylor expansion of the equilibrium current density have been used in Eq. (C1), while Eq. (C4) is correct within the constant-$\tilde{\psi}$ approximation. All the magnetic flux surface averages in Eqs. (C1)–(C4) can be cast in terms of elliptic integrals $E=E[2/(\Omega+1)]$ and $K=K[2/(\Omega+1)]$,

$$\langle 1\rangle_\psi=\frac{4\sqrt{2}}{w\pi}\frac{K}{\sqrt{\Omega+1}}, \tag{C5}$$

$$\langle x\rangle_\psi=1, \tag{C6}$$

$$\langle x^2\rangle_\psi=\frac{w\sqrt{2}}{2\pi}E\sqrt{\Omega+1}, \tag{C7}$$

$$\langle x^3\rangle_\psi=\frac{w^2}{8}\Omega. \tag{C8}$$

These approximations lead to a well defined analytical expression for H',

$$\frac{dH}{d\psi} = v_* \frac{\pi}{w}\left[\frac{\sqrt{2}}{\sqrt{\Omega+1}}\right] \times \left\{ \frac{\frac{C_2}{v_*} - \frac{v}{v_*} + \frac{v}{v_*}\frac{\eta}{D}\frac{w^2}{16}\left[\Omega - \frac{(\Omega+1)E}{K}\right]}{E - \frac{v}{v_*}\frac{\eta}{D}\left(c_b v_* + \frac{v_*^2}{\rho^2}\frac{v}{v_*}\right)\left(E - \frac{\pi^2}{4}\frac{1}{K}\right)} \right\}\Theta. \quad \text{(C9)}$$

Equation (C9) can be used to evaluate the density profile and therefore the bootstrap current contribution to Eq. (23), $-\langle J_b\rangle_\psi/\langle 1\rangle_\psi = c_b(v + H'/\langle 1\rangle_\psi)$. After a straightforward change of variables, Eq. (19) can be written as $\Delta' = 4\int_{-1}^{\infty} d\Omega J \langle \cos(\epsilon y)\rangle_\psi$. Observing that

$$\frac{\langle \cos(\epsilon y)\rangle_\psi}{\langle 1\rangle_\psi} = \frac{(1+\Omega)E - \Omega K}{K}, \quad \text{(C10)}$$

we finally retrieve Eq. (26).

[1] R. J. Buttery, T. C. Hender, D. F. Howell *et al.*, Nucl. Fusion **43**, 69 (2003).
[2] Z. Chang, J. D Callen, E. D Fredrickson *et al.*, Phys. Rev. Lett. **23**, 4663 (1995).
[3] P. H. Rutherford, Phys. Fluids **16**, 1903 (1973).
[4] H. P. Furth, J. Killeen, and M. N. Rosenbluth, Phys. Fluids **6**, 459 (1963).
[5] F. Militello and F. Porcelli, Phys. Plasmas **11**, L13 (2004).
[6] D. F. Escande and M. Ottaviani, Phys. Lett. A **323**, 278 (2004).
[7] R. J. Hastie, F. Militello, F. Porcelli, N. Arcis, M. Ottaviani, D. F. Escande *et al.*, *Proceeding of Invited Paper, 20th IAEA Fusion Energy Conference, Vilamoura Portugal, 2004*, edited by Marianne Spak (IAEA, Vienna, 2004), PD/1-1.
[8] J. R. Hastie, F. Militello, and F. Porcelli, Phys. Rev. Lett. **95**, 065001 (2005).
[9] N. Arcis, D. F. Escande, and M. Ottaviani, Phys. Lett. A **347**, 241 (2005).
[10] N. Arcis, D. F. Escande, and M. Ottaviani, Phys. Plasmas **13**, 052305 (2006).
[11] F. Militello, J. R. Hastie, and F. Porcelli, Phys. Plasmas **13**, 112512 (2006).
[12] W. X. Qu and J. D. Callen, National Technical Information Service Document No. DE6008946, University of Wisconsin, Plasma Report No. UWPR 85-5 (1985).
[13] R. Carrera, R. D. Hazeltine, and M. Kotschenreuther, Phys. Fluids **29**, 899 (1986).
[14] A. I. Smolyakov, Plasma Phys. Controlled Fusion **35**, 657 (1993).
[15] R. Fitzpatrick, Phys. Plasmas **2**, 825 (1995).
[16] H. R. Wilson, J. W. Connor, R. J. Hastie, and C. C. Hegna, Phys. Plasmas **3**, 248 (1996).
[17] M. Ottaviani, F. Porcelli, and D. Grasso, Phys. Rev. Lett. **93**, 075001 (2004).
[18] A. I. Smolyakov, H. R. Wilson, M. Ottaviani, and F. Porcelli, Plasma Phys. Controlled Fusion **46**, L1 (2004).
[19] R. Fitzpatrick, F. L. Waelbroeck, and F. Militello, Phys. Plasmas **13**, 122507 (2006).
[20] F. L. Waelbroeck, J. W. Connor, and H. R. Wilson, Phys. Rev. Lett. **87**, 215003 (2001).
[21] J. W. Connor, F. L. Waelbroeck, and H. R. Wilson, Phys. Plasmas **8**, 2835 (2001).
[22] R. Hazeltine, M. Kotschenreuther, and J. Morrison, Phys. Fluids **28**, 2466 (1985).
[23] R. Fitzpatrick and F. L. Waelbroeck, Phys. Plasmas **12**, 022307 (2005).
[24] B. D. Scott, A. B. Hassam, and J. F. Drake, Phys. Fluids **28**, 275 (1985).
[25] J. Wesson, *Tokamaks*, 3rd ed. (Clarendon, Oxford, 2003), pp. 124–131, *Tokamaks*, 3rd ed. (Clarendon, Oxford, 2003), pp. 166–168.
[26] F. Militello, F. L. Waelbroeck, R. Fitzpatrick, and W. Horton, "Interaction between turbulence and a nonlinear tearing mode in low-beta regime," Phys. Plasmas (submitted).